L-Type Calcium Channel Blockers: From Diltiazem to 1,2,4-Oxadiazol-5-ones via Thiazinooxadiazol-3-one Derivatives

Roberta Budriesi,*[,†] Barbara Cosimelli,*[,‡] Pierfranco Ioan,[†] Maria Paola Ugenti,[†] Emanuele Carosati,[§] Maria Frosini,[||] Fabio Fusi,[||] Raffaella Spisani,[⊥] Simona Saponara,[||] Gabriele Cruciani,[§] Ettore Novellino,[‡] Domenico Spinelli,[⊥] and Alberto Chiarini[†]

Dipartimento di Scienze Farmaceutiche, Università degli Studi di Bologna, Via Belmeloro 6, 40126 Bologna, Italy, Dipartimento di Chimica Farmaceutica e Tossicologica, Università degli Studi di Napoli "Federico II", Via Montesano 49, 80131 Napoli, Italy, Dipartimento di Chimica, Università di Perugia, via Elce di Sotto 8, 06123 Perugia, Italy, Dipartimento di Neuroscienze, Università degli Studi di Siena, Via A. Moro 2, 53100 Siena, Italy, Dipartimento di Chimica Organica "A. Mangini", Università degli Studi di Bologna, Via S. Giacomo 11, 40126 Bologna, Italy

Received October 27, 2008

The research of compounds with L-type calcium channels (LTCCs) blocking activity continued with heterocyclic compounds containing the 1,2,4-oxadiazol-5-one ring. For a series of 22 new derivatives of 3-aryl-4[(*Z*)-(1-methyl-2-alkylsulphanyl-vinyl)][1,2,4]oxadiazol-5(4*H*)-ones, which represent the "frozen" open chain counterpart of the cyclic aryl-thiazinooxadiazolones previously examined, we report here the synthesis and the characterization as LTCC blockers, evaluated on isolated tissues of guinea pig. The most interesting compound, **8b**, was tested also on L-type calcium current recorded in isolated rat tail artery myocytes. Overall, six compounds were more potent than diltiazem, and binding assays confirmed the direct interaction with the benzothiazepine binding site. As the cyclic aryl-thiazinooxadiazolones, *p*-bromine substituted compounds were generally more potent than the corresponding *p*-chlorine ones. A saturated or unsaturated alkyl chain or a bulky group at the sulfur atom were detrimental to the potency, while the compounds with *S*-methyl groups, i.e., thioether (**8b**), sulfoxide (**16a**,**b**), and sulfone (**17b**), gave the best results.

Introduction

The introduction of L-type calcium channel (LTCC[a]) blockers into clinical practice for controlling the activity of mammalian heart dates back to 40 years,[1] but nowadays the role of LTCCs still remains central. The search of new modulators is stimulated by the fact that pathology conditions such as heart failure, one of the most important causes of death in the western world, are related to alterations in Ca^{2+} channel activity.[2]

We described in a previous paper the synthesis and in vitro characterization of a set of 8-aryl-8-hydroxyl-[1,4]thiazino[3,4-*c*][1,2,4]oxadiazol-3-one analogues of diltiazem (DTZ, **1**) (Chart 1), some of which were potent LTCC blockers and selective for the cardiac tissue channel over the vascular one.[3] In particular, compounds nonsubstituted in the 8-phenyl ring (**2**) or substituted with *p*-methoxy (**3**), *p*-chlorine (**4a**), and *p*-bromine (**4b**), were among the most promising. The scaffold of compounds **2**−**4** was further modified,[4] and some structural features were identified to improve the negative inotropic activity. Within the series of thioacetals derived from compounds **4a**,**b**, the most potent compound was **5b** (Chart 1).[4]

Chart 1

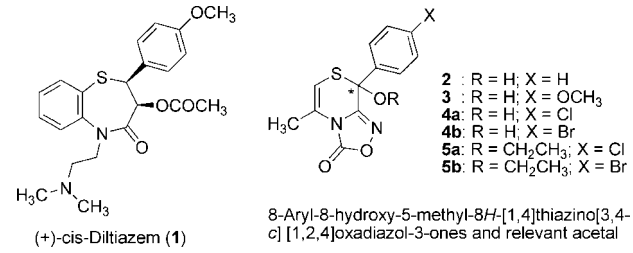

The series of hemithioacetal and thioacetal derivatives, together with other compounds structurally related to **1**,[3−5] were the basis for a 3D-QSAR study[4] and a pharmacophoric model was obtained using GRID molecular interaction fields (MIF).[6] Extracting pharmacologically important regions, a virtual binding site was hypothesized to be composed of three hydrophobic regions and three hydrogen-bonding interactions, one of which reinforced by a charge−charge interaction. Accordingly, a good negative inotropic profile evaluated in the α_1 subunit of the Ca_v1 channels was related to the following structural features in the molecule: one basic center, two or three lipophilic groups, and two hydrogen-bonding (HB) acceptor groups.[7,8] However, not all the pharmacophoric features must be present at once, and missing features can be tolerated. For example, compounds without a basic nitrogen, yet presenting all the other structural features, were expected to fit into the model as well.[4] In fact, for the aforementioned compound **5b**, the binding to the diltiazem site at high concentrations was confirmed experimentally,[9] despite the elimination of the amine moiety. Overall, this

* To whom correspondence should be addressed. For R.B.: phone, +39-051-2099737; fax, +39-051-2099721; E-mail: roberta.budriesi@unibo.it. For B.C.: phone, +39-081-678614; fax, +39-081-678630; E-mail: barbara.cosimelli@unina.it.

† Dipartimento di Scienze Farmaceutiche, Università degli Studi di Bologna.

‡ Dipartimento di Chimica Farmaceutica e Tossicologica, Università degli Studi di Napoli "Federico II".

§ Dipartimento di Chimica, Università di Perugia.

|| Dipartimento di Neuroscienze, Università degli Studi di Siena.

⊥ Dipartimento di Chimica Organica "A. Mangini", Università degli Studi di Bologna.

[a] Abbreviations: LTCC, L-type calcium channel; DTZ, diltiazem; 3D-QSAR, 3D quantitative structure−activity relationships; MIF, molecular interaction fields; HB, hydrogen bonding; ECG, electrocardiogram; HR, heart rate; CPP, coronary perfusion pressure; PR, atrioventricular conduction time; NMR, nuclear magnetic resonance; FLAP, fingerprint for ligands and proteins; DMSO, dimethyl sulfoxide; DMF, *N*,*N*-dimethylformamide; SEM, standard error mean.

10.1021/jm801351u CCC: $40.75
Published on Web 03/26/2009

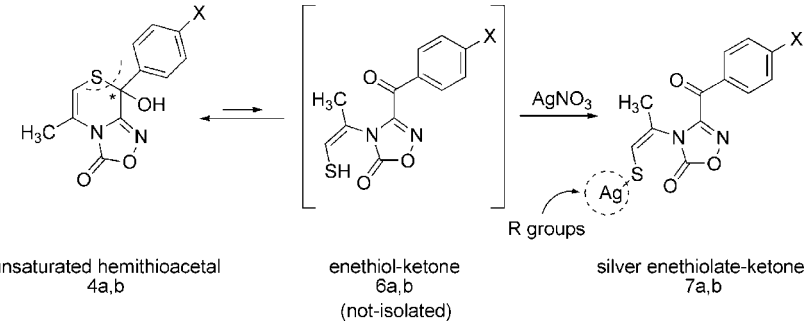

Figure 1. Design strategy for the synthesis of novel compounds. For X, see Charts 1 and 2.

important difference in the chemical structure could strongly affect molecular properties and/or ADME-tox properties such as metabolic stability, cell-permeability, and so on.

Simultaneously to the design of the series presented here, in silico virtual screening procedures were applied to explore the chemical space around the thiazinooxadiazolone and benzothiazepine scaffolds[9,10] and led to the discovery of new interesting hits. Therefore, within the framework of analysis[11] and searching for new chemotypes,[9,10] we are gaining information on variations of structural features responsible for LTCCs-blocking activity.

The analysis of active chemotypes continues here with the examination of another class of heterocyclic compounds containing the 1,2,4-oxadiazole ring: a series of derivatives of 3-aryl-4[(*Z*)-1-methyl-2-(alkylsulphanyl)-vinyl]-[1,2,4]oxadiazol-5(4*H*)-ones, which represent the "frozen" open chain counterpart of the cyclic aryl-thiazinooxadiazolones previously examined.[3,4] Given the equilibrium of the unsaturated hemithioacetals **4a**,**b** with their open chain forms, the aim of this paper is to present the synthesis of a new series of derivatives, assay their LTCCs blocking property in vitro, and compare them with the pharmacophoric information previously extracted for DTZ-like compounds.[4] In particular, 22 new compounds were synthesized and evaluated for their selectivity, potency, and affinity for the LTCCs on different in vitro models, including binding, isolated tissues, and patch-clamp experiments.

Methods

Biology. Functional Studies. The pharmacological profile of all compounds was derived on guinea pig isolated left and right atria to evaluate their inotropic and chronotropic effects, respectively, and on K^+-depolarized (80 mM) guinea pig aortic strips to assess calcium antagonist activity. More precisely, compounds were checked at increasing doses to evaluate the percent decrease of developed tension on isolated left atrium driven at 1 Hz (negative inotropic activity), the percent decrease in atrial rate on spontaneously beating right atrium (negative chronotropic activity), and the percent inhibition of calcium-induced contraction on K^+-depolarized aortic strips (vasorelaxant activity).

The guinea pig isolated perfused heart according to Langendorff was used to assay the whole cardiac activity of the compound precursor of this series (**7b**) in comparison to that of references **1** and **5b**. Compounds were checked at increasing concentrations to evaluate changes in left ventricular pressure (inotropic activity), heart rate (HR; chronotropic activity), coronary perfusion pressure (CPP; coronary activity), and electrocardiogram (ECG) signal.

Data were analyzed using the Student's *t*-test and are presented as the mean ± SEM.[12] Because the compounds were added in a cumulative manner, only the not significance ($P < 0.05$) between the control and the experimental values at each concentration was indicated by an apex letter in the tables. The potency, defined as EC_{50}, EC_{30}, and IC_{50}, was evaluated from log concentration−response curves (Probit analysis by Litchfield and Wilcoxon[12] or GraphPad software[13,14]) in the appropriate pharmacological preparations.

Binding Experiments. Binding assays on rat cardiomyocytes were carried out for the compounds with the most interesting functional profile in order to establish whether they could displace [^{3}H]diltiazem from its binding site.

Electrophysiological Experiments. The most interesting compounds (**4b** and **8b**) were also tested on single smooth muscle cells isolated from the rat tail main artery to assess their LTCCs blocking activity. Compounds were checked at cumulative concentrations to evaluate the percent inhibition of barium current through LTCCs [$I_{Ba(L)}$]. Data are presented as the mean ± SEM. The potency was defined as IC_{50} and evaluated from log concentration−response curves with GraphPad software.[13,14]

Rationale for Drug Design, Chemistry, and Preliminary Findings. Some preliminary chemical considerations are reported below to facilitate the understanding of the design and synthesis (Figure 1) of the compounds in Chart 2. Hemithioacetals are in equilibrium with their thiol-carbonyl open chain forms, recalling the situation occurring in hemiacetals. The cyclic forms are stable as five- or six-member rings. In contrast, the equilibrium is predominantly, or even completely, shifted toward the open chain form in the case of noncyclizable compounds or not-stable cyclic compounds. Moreover, it is well-known that both −O-C_{sp3}− and −S-C_{sp3}− bonds of the acetal or thioacetal type are quite weak.[15] This is demonstrated by the behavior of the cyclic hemiacetal α-D-glucopyranose, stable in the solid state but able to give slow spontaneous or fast acid-catalyzed enantiomerization in water and to react easily with phenylhydrazine.[16,17] Finally, it should be recalled that the −S-C− bond is significantly weaker than the −O-C− bond (the energy difference being about 20 kcal mol^{-1}).[15]

Thus, in cyclic hemithioacetals the addition of a reagent capable of "capturing" thiols (e.g., giving an insoluble derivative) completely shifts the equilibrium toward the open chain form. The optimal reagents could be inorganic salts soluble in the reaction conditions used, such as the salts of heavy metals (silver, mercury, or lead),[18] capable of forming insoluble thiolates. On the contrary, salts of calcium, magnesium, and so on do not work for the ring opening of **4a**,**b**, whereas silver nitrate appears to be the first choice reagent. It is soluble in water as well as in ethanol, it is easy to use, and it can form thiolates that are insoluble in both water and ethanol. Moreover, silver salts are less toxic than mercury or lead ones and behave as good nucleophiles with haloalkanes, or generally speaking, with reactive organic halides,[19−21] giving the relevant sulfides via a Williamson-like synthesis.[22]

Chart 2

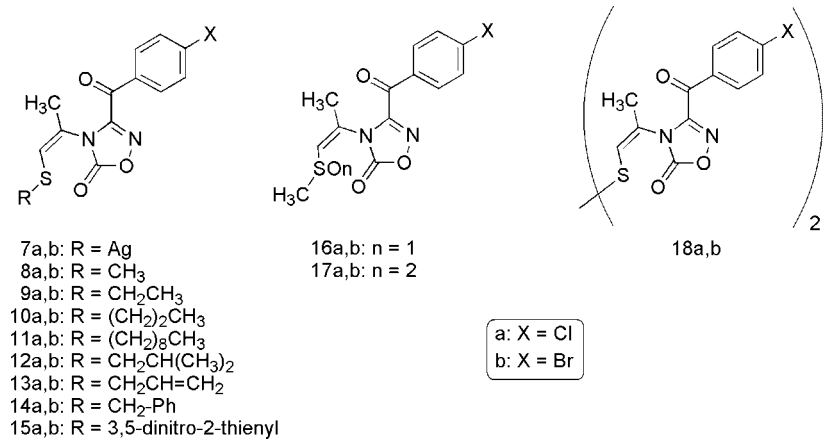

On the basis of the considerations given above, preliminary studies have been carried out on compounds **4a**,**b** and **7a**,**b** in order to monitor the activity on the calcium channel and to extend the cardiovascular profile. First, we carried out experiments on rat cardiomyocytes with [^{3}H]diltiazem. Among the previously examined hemithioacetals,[3] one of the compounds exhibiting the most potent negative inotropic effect, namely **4b**, was considered (for data see Table 1). The direct interaction of **4b** with the binding site of **1** was confirmed to cause a concentration-dependent inhibition of [^{3}H]diltiazem binding with a K_i of 0.29 μM, while the K_i of **1** was 0.085 μM. The comparison of effects of **1** and **4b** on [^{3}H]diltiazem binding is evidenced in Figure 2.

Opening the 1,4-thiazino ring of **4a**,**b** (Scheme 1) with silver nitrate, the starting compounds were "frozen" in their open chain forms and the silver thiolates **7a**,**b** were obtained. Their cardiovascular profile strictly recalls that of the cyclic hemithioacetals **4a**,**b** for the weak chronotropic and vasorelaxant effects (Table 1). In particular, **7a**,**b** and **4a**,**b**[3] did not show significant negative chronotropic activity and also their vasorelaxant effects were lower than 30%.

In contrast, a biphasic profile concerned the inotropic activity (Figure 3): **7a**,**b** show negative inotropic activity at low concentrations (<50% at 10^{-6} M) (Table 1), and positive inotropic activity at high concentrations, gaining a δ of $+60 \pm 2.4$ in the interval $10^{-6}-10^{-4}$ M (**7a**) and $+33 \pm 1.9$ in the interval $10^{-6}-10^{-5}$ M (**7b**) from control.

The behavior of **7a**,**b** proves the negative inotropic effect of open chain compounds (Table 2), whereas the positive inotropic effect, observed at higher dosages, could be related, in some way, to the presence of the silver cations, known to induce contraction controlled by LTCC, thus hiding the negative inotropic activity.[23] In addition, these cations induce calcium release from the sarcoplasmic reticulum in vitro by acting on the calcium release channel and the calcium pump.[24] The Langendorff data for **7b**, which is a weak LTCCs blocker at low concentrations (up to 10^{-6} M, see Table 1), support the hypothesis of the positive inotropic effect due to the presence of silver cations.

Given these preliminary results, we designed the series of sulfides presented in Chart 2 via the Williamson-like reaction, linking to the sulfur atom short and long unbranched (**8a**,**b**−**11a**,**b**) or branched (**12a**,**b**) alkyl chains, an unsaturated and unbranched chain (**13a**,**b**), the benzyl group (**14a**,**b**), and the 3,5-dinitrothiophen-2-yl residue (**15a**,**b**). The nitro group has been introduced in compounds **15a**,**b** because it is likely a key feature for the LTCCs blocking activity of drugs such as nifedipine, largely used in cardiovascular therapy.[1] The sulfoxide and the sulfone moiety have been introduced in **16a**,**b** and **17a**,**b**, respectively, on the basis of some hits of recent virtual screening studies[9,10] and other known LTCC blockers.[25,26] Finally, to

Table 1. The Effect on Cardiac Activity Evaluated in Isolated Perfused Guinea Pig Spontaneously Beating Heart of **7b** and Reference Compounds **1** and **5b**

compd		% change[a]	pEC_{50}(95% cl)[b]
1	+(d*P*/d*t*)max[d]	−59 ± 4.2	8.03 (8.21−7.90)
	HR[e]	−25 ± 1.9	
	CPP[f]	−51 ± 3.1	7.66 (7.80−7.03)
	PR[g]	+34 ± 2	
5b[c]	+(d*P*/d*t*)max[d]	−3 ± 0.2[h]	
	HR[e]	−14 ± 0.8	
	CPP[f]	−9 ± 0.5	
	PR[g]	+32 ± 1.6	
7b	+(d*P*/d*t*)max[d]	0	
	HR[e]	−4[h]	
	CPP[f]	−3[h]	
	PR[g]	+30	

[a] Percentage change of the basal value at the highest concentration tested (1 μM). Each value corresponded to the mean ± SEM. [b] $pEC_{50} = -\log EC_{50}$ calculated from log concentration−response curves (GraphPad Prism Software,[13,14] $n = 4-6$); cl, confidential limits. [c] Data from ref 4. [d] +(d*P*/d*t*)max: maximal rate of the increase in left ventricular pressure. [e] HR: heart rate calculated from ECG signal. [f] CPP: coronary perfusion pressure. [g] PR: atrio−ventricular conduction time. [h] $P < 0.05$.

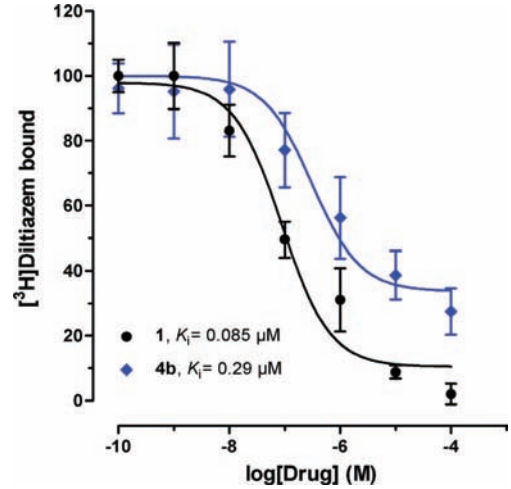

Figure 2. Effects of **1** and **4b** on [^{3}H]diltiazem binding. Each point is the mean ± SEM ($n = 5-8$).

Scheme 1[a]

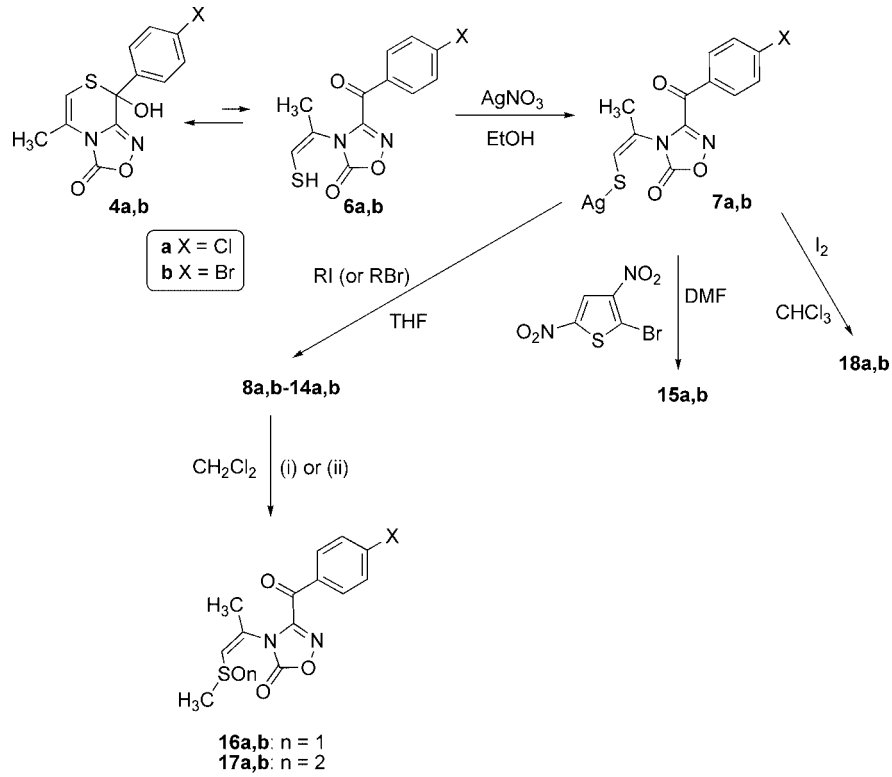

[a] (i) **8a** or **8b** (1 equiv) MCPBA (1 equiv), to obtain **16**; (ii) **8a** or **8b** (1 equiv) MCPBA (2 equiv), to obtain **17**.

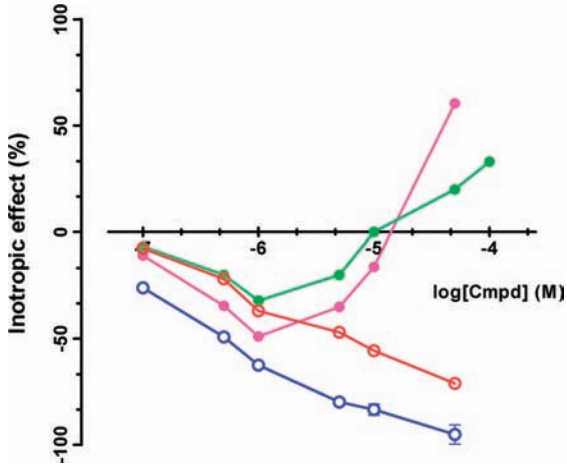

Figure 3. Inotropic profile of compounds **7a** (magenta), **7b** (green), **8a** (red), and **8b** (blue) on guinea pig left atria driven at 1 Hz. Values are mean ± SEM (n = 5−6). Where error bars are not shown, these are covered by the point itself.

investigate the effect on the activity of duplicating the structure of **6a**,**b**, the disulfides **18a**,**b** were designed.

The synthetic strategies of all the above-mentioned compounds are summarized in Scheme 1, which shows the new 1,2,4-oxadiazol-5-ones obtained. As discussed above, the cyclic compounds **4a**,**b** are in equilibrium with the relevant open chain forms **6a**,**b**, the equilibrium being largely shifted toward the cyclic form, as suggested by the known general behavior of six-membered ring cyclic hemithioacetals and confirmed by X-rays measurements and NMR data.[27,28]

In all of the synthesized sulfides, the *Z*-isomer is always obtained, except in the instances of **12a**,**b**. For these, a small amount of the *E*-isomer has been isolated, probably because of the hindrance of the isobutyl chain.

The sulfoxides **16a**,**b** and the sulfones **17a**,**b** were obtained by starting from methansulphanyl derivatives **8a**,**b** by simple oxidation with one or two equivalents, respectively, of 3-chloroperbenzoic acid.

Results

Structure−Activity Relationships. For the new compounds **7a**,**b**−**18a**,**b**, the results of negative inotropy and chronotropy as well as vasorelaxant activity are summarized in Table 2. Diltiazem (**1**) and the previously mentioned 1,2,4-oxadiazol-3-ones (**2**−**5a**,**b**) were used as reference, while the determined functional activity is expressed as efficacy and potency.

At first sight, the biological data indicates that, in line with the predicted values, the new series mimics the activity profile of the previously examined cyclic compounds.[3] For the set of compounds **8a**,**b**−**18a**,**b**, only significant negative inotropic activity was observed, while chronotropic and vasorelaxant activities were always below the value of 50%. Concerning the inotropic activity, the behavior of all the compounds recall that of **8a**,**b** (see Figure 3), which do not present positive inotropic effect. This supports our hypothesis about silver cations for the above-mentioned reasons.

From the analysis of the series with linear saturated chains (**8a**,**b**−**11a**,**b**), the most potent compound results to be **8b** (EC_{50} = 0.41 μM c.l. 0.29−0.56), which has the 4-bromine substituent in the phenyl ring and the shortest alkyl chain (X = Br; R = CH_3). An overview of the potency of the series is given in Figure 4: it clearly shows that usually bromo-containing compounds are significantly more active than the chloro containing ones.

Compounds **9b**, **10b**, and **11b**, containing slightly longer alkyl chains as ethyl and propyl groups, or a longer linear saturated chain (*n*-nonyl group), are equipotent and less potent compounds than **8b** (EC_{50} = 1.33 μM c.l. 0.99−1.72; EC_{50} = 1.22 μM c.l. 0.82−1.63; EC_{50} = 1.03 μM c.l. 0.85−1.33; EC_{50} = 0.41 μM

Table 2. Cardiovascular Activity of Tested Compounds

compd	% decrease (M ± SEM)		EC_{50} of negative inotropic activity		vasorelaxant activity
	negative inotropic activity[a]	negative chronotropic activity[b]	EC_{50}[c] (μM)	95% conf lim($\times 10^{-6}$)	activity[d] (M ± SEM)
1[e]	78 ± 3.5[h]	94 ± 5.6[k]	0.79	0.70−0.85	88 ± 2.3
2[f]	95 ± 3.2[h]	14 ± 0.5[i]	0.23	0.18−0.30	4 ± 0.2[i,l]
3[f]	97 ± 3.7[i]	18 ± 1.0[i]	0.32	0.23−0.43	12 ± 0.6[i]
4a[f]	80 ± 4.1[h]	18 ± 1.8[i]	0.80	0.65−1.05	26 ± 1.4[i]
4b[f]	97 ± 3.7[i]	18 ± 1.0[i]	0.32	0.23−0.43	12 ± 0.6[i]
5a[g]	53 ± 0.6[j]	16 ± 0.2[i]	0.27	0.14−0.45	28 ± 1.4[i]
5b[g]	77 ± 1.7[i]	5 ± 0.2[h,l]	0.04	0.03−0.05	19 ± 0.9[i]
7a	49 ± 2.4[k]	7 ± 0.5[l]			4 ± 0.2[l]
7b	32 ± 1.6[k]	18 ± 0.8[k]			26 ± 2.1
8a	71 ± 1.9[i]	10 ± 0.9[i]	1.45	1.22−1.70	8 ± 0.6[i,l]
8b	95 ± 4.5[i]	2 ± 0.1[h,l]	0.41	0.29−0.56	10 ± 0.9
9a	75 ± 0.1[i]	30 ± 1.5[i]	2.09	1.95−2.36	27 ± 1.3
9b	89 ± 2.7	18 ± 1.4	1.33	0.99−1.72	43 ± 2.5
10a	84 ± 3.2	17 ± 1.4[i]	2.19	1.94−2.35	15 ± 1.3
10b	80 ± 4.7	10 ± 0.7	1.22	0.82−1.63	26 ± 1.3
11a	84 ± 1.1[h]	2 ± 0.1[l]	0.67	0.44−0.80	5 ± 0.2[l]
11b	84 ± 3.7	3 ± 0.2[l]	1.03	0.85−1.33	12 ± 0.2
12a	84 ± 1.2	5 ± 0.2[l]	2.07	1.88−2.47	6 ± 0.1[l]
12b	88 ± 1.4	16 ± 1.1	0.91	0.59−1.41	24 ± 1.4
13a	70 ± 3.5	6 ± 0.3[j]	1.35	0.93−1.72	23 ± 1.6
13b	89 ± 4.2	18 ± 0.9[i]	1.29	0.87−1.36	21 ± 1.3
14a	78 ± 0.6	5 ± 0.4[l]	1.55	1.09−1.97	33 ± 1.9
14b	80 ± 3.1[i]	31 ± 2.5[h]	1.28	0.95−1.73	6 ± 0.5[i,l]
15a	67 ± 1.4[i]	15 ± 0.3[i]	1.42	1.21−1.68	35 ± 1.4[i]
15b	85 ± 3.2[j]	27 ± 1.5[h]	0.73	0.51−1.03	32 ± 1.7[i]
16a	71 ± 2.2[i]	4 ± 0.1[l]	0.21	0.18−0.26	7 ± 0.6[l]
16b	89 ± 1.8	33 ± 2.1	0.48	0.34−0.69	2 ± 0.1[l]
17a	72 ± 3.4	7 ± 0.2[l]	1.11	0.87−1.41	13 ± 0.7
17b	73 ± 2.4[i]	7 ± 0.2[j,l]	0.28	0.21−0.39	6 ± 0.3[i,l]
18a	72 ± 4.5	4 ± 0.1[l]	4.39	3.22−4.87	6 ± 0.4[l]
18b	73 ± 4.2	9 ± 0.3[l]	1.70	1.19−2.01	5 ± 0.2[l]

[a] Decrease in developed tension in isolated guinea-pig left atrium at 10^{-4} M, expressed as percent changes from the control ($n = 4-6$). The left atria were driven at 1 Hz. 10^{-4} M gave the maximum effect for most compounds. [b] Decrease in atrial rate on guinea-pig spontaneously beating isolated right atrium at 10^{-4} M, expressed as percent changes from the control ($n = 6-8$). Pretreatment heart rate ranged from 165 to 190 beats/min. 10^{-4} M gave the maximum effect for most compounds. [c] Calculated from log concentration−response curves (Probit analysis by Litchfield and Wilcoxon with $n = 6-7$).[12] When the maximum effect was <50%, the EC_{50} ino., EC_{30} chrono., IC_{50} of vasorelaxant potency values were not calculated. [d] Percent inhibition of calcium-induced contraction on high potassium-depolarized guinea-pig aortic strip at 10^{-4} M ($n = 5-6$). 10^{-4} M gave the maximum effect for most compounds. [e] $EC_{30} = 0.07$ μM (c.l. 0.064−0.075), $IC_{50} = 2.6$ μM (c.l. 2.2−3.1). [f] Data from ref 3. [g] Data from ref 4. [h] At 10^{-5} M. [i] At 5×10^{-5} M. [j] At 5×10^{-6} M. [k] At 10^{-6} M. [l] $P < 0.05$.

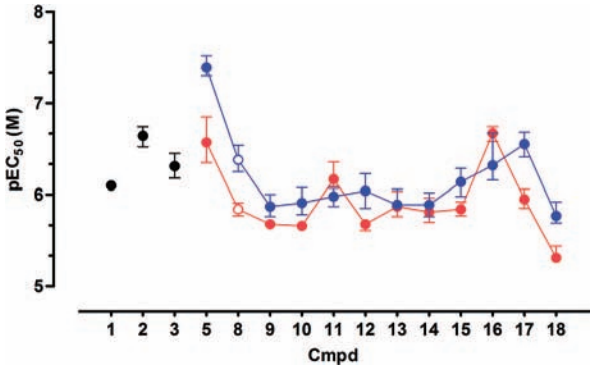

Figure 4. For the references **1**, **2**, **3**, and **5a**,**b** and for all the compounds of the series, the pEC_{50} values are indicated in red for *p*-chlorine (**a**) and blue for *p*-bromine (**b**). Open circles are used for **8a** (red) and **8b** (blue). Each point and vertical bar represents the mean ± 95% confidential limits ($n = 5-7$). Where error bars are not shown, these are covered by the point itself.

c.l., 0.29−0.56, respectively). Despite the trend observed for the acetals of thiazinooxadiazol-3-ones,[4] in this case the longer linear saturated chain does not affect significantly the potency of compounds. This evidence supports the hypothesis of different positions within the binding site of the two groups, −OR and −SR, for acetals of thiazinooxadiazol-3-ones (as **5b**) and sulfides of oxadiazol-3-ones (**8a**,**b**−**13a**,**b**), as discussed in the next section.

Further support comes from the comparison of compounds **12a**,**b**−**15a**,**b**. Compound **12b**, containing the isopropyl residue, shows a negative inotropic potency comparable to those of the compounds mentioned above, whereas introducing a short unsaturated chain (the allyl group of compounds **13a**,**b**) only affects the potency marginally. Furthermore, not only do all these compounds show similar activity and potency, but a large variation (increase) of the steric requirements does not change the situation. In fact, compounds **14a**,**b** containing a benzyl group showed a potency similar to that of the other compounds with different chains, whereas compounds **15a**,**b** with the bulky 3,5-dinitrothiophen-2-yl group have a slightly better potency.

The results of recent virtual screening experiments, where large databases were searched to discover new chemotypes as LTCC blockers, suggested that the sulfonyl group represents an interesting pharmacophore for LTCC blockers activity;[9,10] this is confirmed here by the biological data of the sulfones (**17a**,**b**). In addition, the sulfoxide **16a** is equipotent with **17b**: they are the two most potent compounds presented in this study.

These results deserve further future examination, due to the following peculiarities: (i) in the pair **16a**,**b**, the chlorine derivative is more potent than the bromine derivative; (ii) the sulfoxide group is chiral at the sulfur atom; (iii) electronic effects of the two groups (−SO− and $-SO_2-$) are "different", as supported by their substituent constants. In fact, comparing *meta* and *para* Hammett constants, one can find significant differences

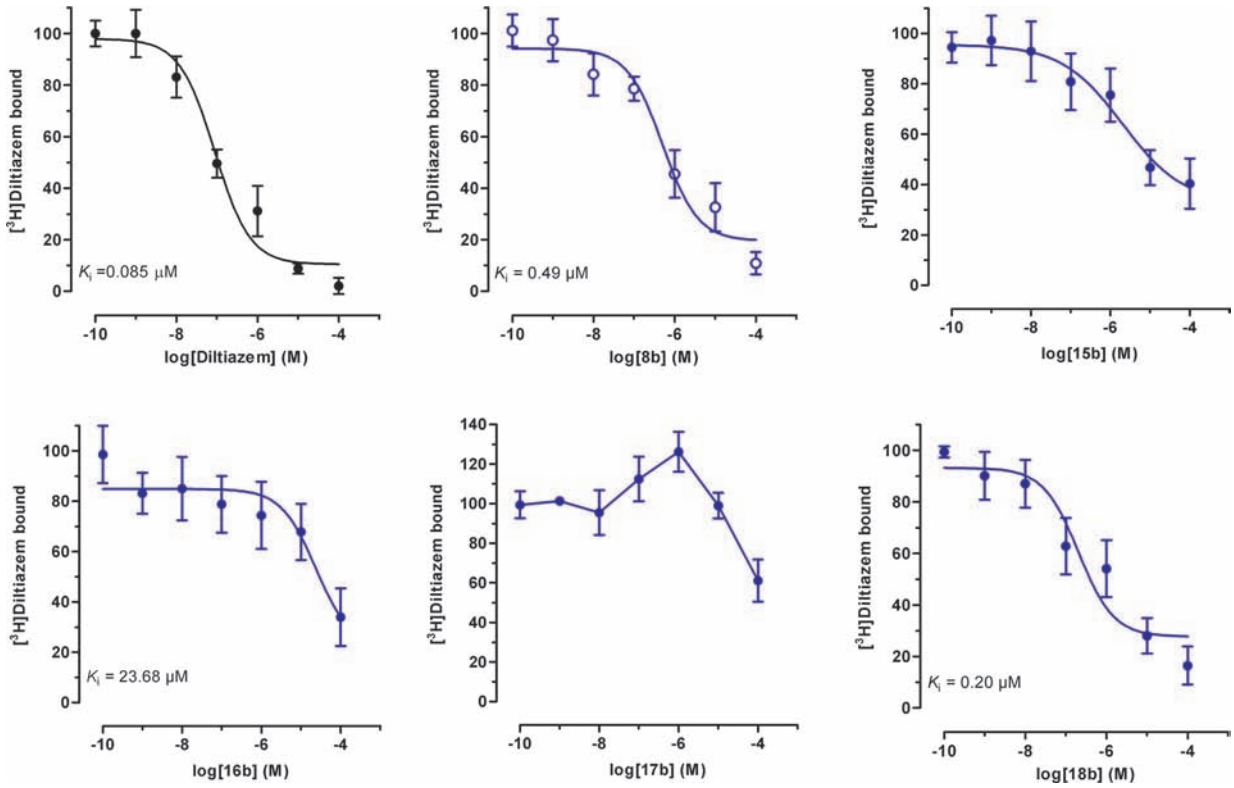

Figure 5. Effects of compounds Diltiazem, **8b**, **15b**, **16b**, **17b**, and **18b** on [^{3}H]diltiazem binding. Each point is the mean ± SEM (n = 7−9).

in their absolute values and different inductive and mesomeric contributions to the global electronic effects, being $\sigma_p < \sigma_m$ in the case of $-SOCH_3$ and $\sigma_p > \sigma_m$ in the case of $-SO_2CH_3$.[29]

In summary, the significant variation in the chemical structure produced by introducing SO or SO_2 groups could be responsible for a different orientation of **16a**,**b** and **17a**,**b** within the binding site, as detailed in the Discussion Section.

Finally, compounds **18a**,**b** are peculiar because they duplicate the main scaffold through the disulfide bond. Their particular structure corresponded, for the chlorine derivative **18a**, to the lowest potency value of the series.

Binding Studies. For some selected compounds, binding assays on rat cardiomyocytes were carried out in order to confirm their binding site. [^{3}H]Diltiazem (5 nM) was incubated with increasing concentrations (0.1 nM to 100 μM) of the ligands as described in the Supporting Information. Data presented in Figure 5 report the effect of the reference **1** and of compounds **8b**, **15b**, **16b**, **17b**, and **18b** on [^{3}H]diltiazem.

Compound **8b** (Figure 5) caused a concentration-dependent inhibition of [^{3}H]diltiazem binding, with a K_i of 0.49 μM. This value was not significantly different from results obtained with **4b** (see Figure 2) and thus supporting the hypothesis of a common binding site. Compound **15b** shares the same binding site as well but with markedly lower affinity.

It is worthwhile to note that the groups $-SCH_3$ of **8b** and $-SOCH_3$ of **16b** (Figure 5) produced the same binding profile, although the K_i of **16b** was about 2 orders of magnitude higher than that of **8b**, indicating a strong decrease in affinity. Much more interestingly, the $-SO_2CH_3$ group of **17b** corresponded to a complete change in the interaction with the benzothiazepine site. Indeed, compound **17b** displayed a complex interaction with the benzothiazepine binding site. A small stimulation of [^{3}H]diltiazem binding (~25%) produced at 1 μM was followed by partial inhibition at higher concentrations. This behavior has been already observed for compound **5b**,[9] which is more potent than **17b** in stimulating the binding of [^{3}H]diltiazem.

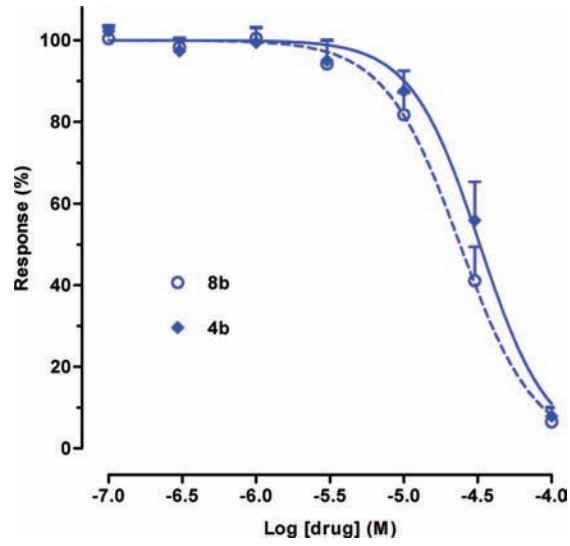

Figure 6. Effects of compounds **4b** and **8b** on $I_{Ba(L)}$ (5 mM Ba^{2+}, 0 mV, V_h = −80 mV). Each point is the mean ± SEM (n = 5−6). Where error bars are not shown, these are covered by the point itself.

Finally, the binding profile observed for **18b** recalled that of **8b** (Figure 5). The hydrolysis of the disulfide bond was hypothesized as responsible for such a profile, but other experimental evidence is needed to verify such hypothesis.

Results from Electrophysiological Experiments. Finally, the effect of compounds **4b** and **8b** on $I_{Ba(L)}$ recorded in vascular myocytes was assessed in order to provide direct evidence of their LTCC blocking activity (Figure 6). Both compounds were almost completely ineffective up to 10 μM concentration. At higher concentrations, compounds **4b** and **8b** inhibited peak $I_{Ba(L)}$ in a concentration-dependent manner, with IC_{50} values of 33.36 ± 5.95 μM (n = 4) and 25.21 ± 4.78 μM (n = 4), respectively. Taken together, the electrophysiological and binding data proved

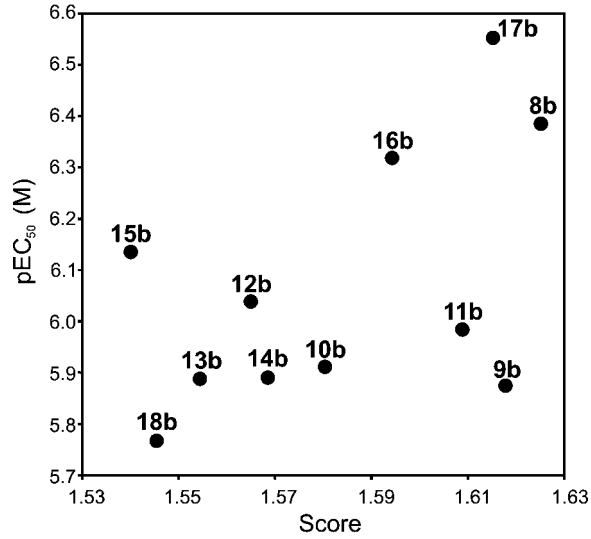

Figure 7. Scores obtained for the compounds **8b**−**18b** compared with the pEC_{50} values. For compound **5b**, not shown here, the score obtained was 1.57.

the direct interaction of compounds **4b** and **8b** with the pore-forming subunit of LTCCs. Furthermore, the IC_{50} values, being 100- and 60-fold higher, respectively, than the corresponding EC_{50} value for negative inotropic activity, supported once more their cardioselective LTCCs blocking activity.

Discussion

The design of this series of compounds reflected the choice of the R substituents. Reasonable considerations came from classic structure−activity relationships previously observed for the alcoholic group (see R in Chart 1) and from pharmacophoric information derived in the same work.[4] Accordingly, not too bulky and prevalently lipophilic R substituents were selected. However, the series' inotropic profile discussed above (see Figure 4) clearly shows that only the introduction of the small methyl group provided interesting potency values (below 0.5 μM), whereas the steric obstruction, occurring for any larger substituent linked to the sulfur atom, was most likely responsible for the weaker potency.

One of the main focuses of in silico procedures applied to drug discovery processes is to provide hypotheses for understanding which molecular features are important or detrimental for biological activity. Computational approaches applied to study the channel−ligand interaction, because of the not-negligible flexibility of the channel and of its ligands, could produce for the same compound hypothetical not-unique binding modes, as already proposed by Tikhonov and Zhorov for an analogue of **1** on the basis of a recent structure-based approach.[30]

In the present paper, a ligand-based approach has been applied: as in a ligand-based virtual screening procedure, compound **1** was selected as molecular template and a similarity measure versus **1** was calculated for all the molecules of this series. The scores measuring such similarity are reported for the compounds **8b**−**18b** in Figure 7 and compared to the pEC_{50} values in order to prove the validity of such method.

An additional result of this approach is the 3D superposition over **1**, obtained using the FLAP program,[31] reported here for only some compounds. The final goal of this ligand-based application was not to claim a definitive orientation within the LTCC diltiazem binding site but to discuss one of their possible orientations with respect to **1** in order to facilitate the comprehension of the experimental data.

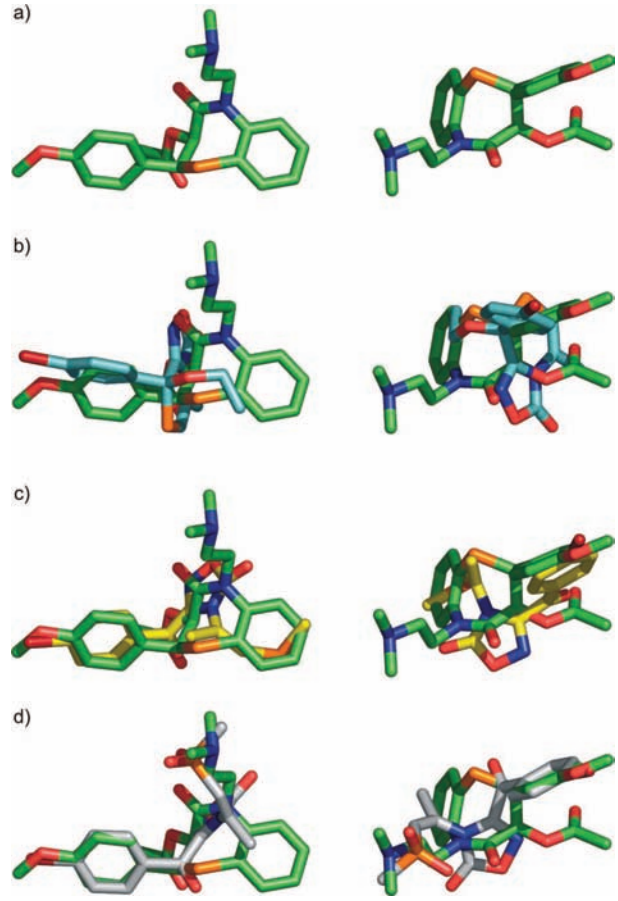

Figure 8. Two different views for the three-dimensional structure of **1** (a) and the 3D-superimpositions of **5b** (b), **8b** (c), and **17b** (d) over **1**. The compounds are color-coded as follows: oxygen atoms are red, sulfur atoms are gold, nitrogen atoms are blue, bromine atoms are dark-red; carbon atoms are green for **1**, cyan for **5b**, yellow for **8b**, and light-gray for **17b**. Hydrogen atoms are not shown for clarity. The figure was prepared using PyMol.[32]

Some ligand molecules were selected among the series, namely **5b**, **8b**, and **17b**. For each pair template−ligand molecule, i.e., **1**−**5b**, **1**−**8b**, and **1**−**17b**, two different views of such 3D-superpositions (of **5b**, **8b**, **17b** over **1**) are given in Figure 8 and discussed below.

Overall, **1** presents one large hydrophilic region and two hydrophobic moieties, the *p*-substituted phenyl and the benzo-fused rings (see Figure 8a and Figure 9). Three oxygen atoms of **1** are responsible for a large hydrophilic region in the central part of the molecule over which the 1,2,4-oxadiazol-5-one moiety of **5b**, **8b**, and **17b** is aligned, even if with different orientations. The GRID MIF, used by FLAP for the alignment, are reported in Figure 9 for compounds **1** and **8b** in order to highlight the steric, hydrophobic, and hydrophilic interactions of the two compounds.

According to the alignment proposed, the *p*-substituted ring of all the four compounds lies in the same region, while different groups lie in correspondence of the benzo-fused ring of **1** for the three ligands considered. For compound **5b** the position of the $-OCH_2CH_3$ chain suggests that there is space enough to fit in the same position larger groups (Figure 8b), in agreement with recently published experimental evidence.[4] A more "reduced" space is available for compound **8b** (Figure 8c), whose $-SCH_3$ group fits over the benzo-fused ring. This orientation is in agreement with experimental results of the series presented here, which suggests the small methyl group as the best

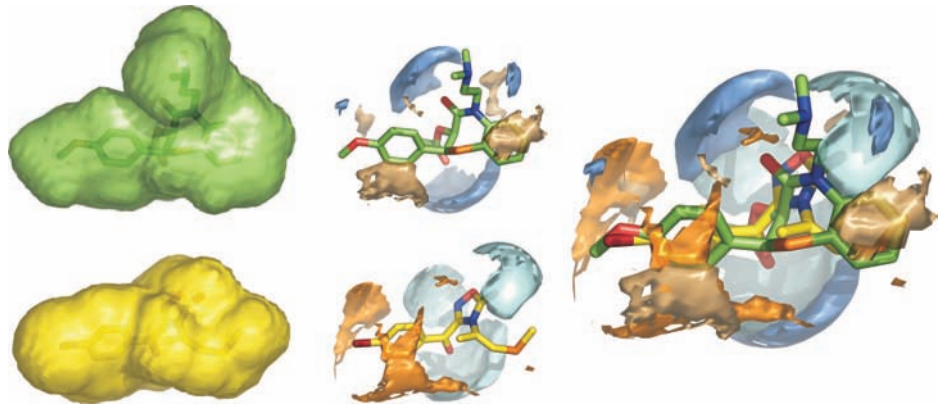

Figure 9. Steric, hydrophobic, and hydrophilic interactions are reported for compounds **1** and **8b**. Green surface (for **1**) and yellow surface (for **8b**) were obtained plotting the GRID fields for the OH2 probe at +0.5 kcal/mol. In addition, the hydrophobic fields (obtained with the GRID probe at −0.8 kcal/mol) are reported in gold (for **1**) and orange (for **8b**), whereas the hydrophilic fields (obtained with the GRID probe at −4.0 kcal/mol) are reported in blue (for **1**) and cyan (for **8b**). The superimposition proposed for the two compounds (see Figure 8c) is also reported with all the fields. The figure was prepared using PyMol.[32]

substituent at the sulfur atom. Longer chains could result in a overoccupance of the benzo-fused region, causing a steric hindrance with the binding site. Finally, the orientation proposed for **17b** allowed supposition of a binding mode different from **8b** because the sulfur oxidation changes the character of such portion of molecule that is better aligned, for shape and type of interaction, with the *N*-chain of **1**. Of course, this different orientation implies different forces to drive the binding process. According to the hypothesis of Figure 8d, a reduced affinity of the hydrophobic moieties is counterbalanced by a new channel−ligand interaction that occurs in correspondence of the basic nitrogen of **1**. In fact, the sulfone group of **17b** could participate in a ternary complex with a calcium ion and the channel, as recently proposed by Tikhonov and Zhorov for the carbonyl oxygen of **1**.[30] Further experiments are necessary to clarify this point and verify such hypothesis.

Conclusion

The synthesis and characterization as LTCC blockers of 22 new compounds presented in this paper are part of a wider project aimed at discovering new potent and selective LTCC blockers via experienced synthetic strategies combined with in silico and in vitro techniques.

Therefore, the examination of compounds with different chemical structures was continued with the analysis of the 1,2,4-oxadiazol-5-ones presented here. To gain further information on the inotropic activity of these open chain compounds, we have taken advantage of the reactivity of silver salts **7a**,**b** with compounds able to undergo attack from nucleophiles.

The study of these new LTCC blockers **7**−**18a**,**b**, carried out through in vitro functional assays, showed that the new series mimic the activity profile of the previously examined cyclic compounds:[3] only significant negative inotropic activity was observed, whereas chronotropic and vasorelaxant activities were always below the value of 50%. Such selective negative inotropic compounds could be helpful in the treatment of hypertension obstructive cardiomyopathy (HOCM), known also as idiopathic stenosis as previously described.[10,33−35]

Concerning the inotropic profile, compounds **8b**−**18b** were more potent than **8a**−**18a**, as it has already been observed for the thiazino-oxadiazolones. Among the 11 couples of compounds, **11** and **16** were the only cases in which *p*-chlorine compounds are more potent than the corresponing *p*-bromine ones. However, for **11a**,**b**, the variation in terms of inotropic potency was so close to the experimental errors that no speculation could be made, whereas for **16a**,**b**, this and other points require further examination.

Neither the length of alkyl chain nor a bulky group linked to the sulfur atom affected the potency, the most likely reason being that the alkyl chain is accommodated within the receptor site in a small pocket. Thus, significant changes in chain length cause only modest and not significant variation of the potency. On the contrary, the introduction of a strong electron-withdrawing group, as in compounds **16a**,**b** and **17a**,**b**, where the sulfide moiety has been oxidized to sulfoxide or sulfone, caused an increase of the activity and a different profile arose by binding experiments with [^{3}H]diltiazem. The change in the electron density of this portion of the molecule is likely responsible for the peculiar interactions with the receptor site, as hypothesized using 3D in silico methods.

Experimental Section

A. Chemistry. General. ^{1}H and ^{13}C NMR spectra were recorded on a Varian Gemini 300 Instrument in the Fourier transform mode at 21 (±0.5 °C) in DMSO-d_6. Chemical shifts (δ) are in parts per million (ppm) from tetramethylsilane, and coupling constants are in Hz. ESI-MS were registered on a Micromass ZMD Waters instrument (30 V, 3.2 kV, isotopes observed ^{35}Cl and ^{79}Br). HRMS were recorded on a Thermo Finnigan Mat95XP apparatus (isotopes observed ^{35}Cl and ^{79}Br). Details concerning spectrometric measurements are reported in the Supporting Information. Melting points were determined on a Kofler apparatus and are uncorrected. Solvents were removed under reduced pressure. Silica gel plates (Merck F_{254}) and silica gel 60 (Merck 230−400 mesh) were used for analytical TLC and for column chromatography, respectively. Compounds **4a**[27,28] and **4b**[36] were obtained as previously reported. Accurate ^{1}H NMR spectra and analytical TLC ensure for all of the new tested compounds a purity degree >98%. All new compounds gave satisfactory microanalyses (C, H, N, and S; not reported). Melting points, yields, reaction times, and HRMS are collected in Table 3. Detailed ^{1}H and ^{13}C NMR spectra of all compounds are reported in the Supporting Information.

Silver (1*Z*)-2-[3-(4-Halogenobenzoyl)-5-*oxo*-1,2,4-oxadiazol-4(5*H*)-yl]prop-1-ene-1-thiolates (7a,b). A solution of $AgNO_3$ (1.9 mmol) in ethanol (17 mL) was added dropwise to a solution of **4a** or **4b** (1.5 mmol) in ethanol (17 mL) under magnetic stirring at room temperature. The white precipitate formed was collected, dried under vacuum, and taken in the dark.

General Procedure for the Synthesis of 3-(4-Halogenobenzoyl)-4[(*Z*)-2-(alkylthio)vinyl-1-methyl]-1,2,4-oxadiazol-5(4*H*)-

Table 3. Reaction Times, Yields, Melting Points, and HRMS Concerning **7a**,**b**−**18a**,**b**

no.	X	R	*n*	time (h)	yield (%)[a]	mp (°C)	HRMS calcd/found
7a	Cl	Ag			82	120−144 (dec)	
7b	Br	Ag			73	123−136 (dec)	
8a	Cl	CH_3		26	76	139−140	310.0174/310.0179[b]
8b	Br	CH_3		27	75	160−161	353.9670/353.9674[c]
9a	Cl	CH_3CH_2		26	29	87−89	324.0333/324.0335[b]
9b	Br	CH_3CH_2		22	36	94−96	367.9834/367.9830[c]
10a	Cl	$CH_3CH_2CH_2$		20	24	57−58	338.0495/338.0492[b]
10b	Br	$CH_3CH_2CH_2$		26	16	yellow oil	381.9983/381.9987[c]
11a	Cl	$CH_3(CH_2)_7CH_2$		4	92	57−58	422.1431/422.1430
11b	Br	$CH_3(CH_2)_7CH_2$		4	89	70−71	466.0926/466.0924
12a	Cl	$(CH_3)_2CHCH_2$		4	58		352.0648/352.0648
12b	Br	$(CH_3)_2CHCH_2$		4	64		396.0143/396.0145
13a	Cl	$CH_2{=}CHCH_2$		24	52	71−72	336.0331/336.0335[b]
13b	Br	$CH_2{=}CHCH_2$		24	57	93−94	379.9837/379.9830[c]
14a	Cl	$C_6H_5CH_2$		28	51	122−123	386.0495/386.0492[b]
14b	Br	$C_6H_5CH_2$		28	50	127−128	429.9986/429.9987[c]
15a	Cl	3,5-dinitro-2-thienyl		144	18	202−204	467.9605/467.9601[b]
15b	Br	3,5-dinitro-2-thienyl		144	29	205−206	511.9091/511.9096[c]
16a	Cl		1	1.5	73	173−174	326.0125/326.0128
16b	Br		1	6	75	196−198	369.9629/369.9623
17a	Cl		2	3	65	192−194	342.0078/342.0077[b]
17b	Br		2	3	80	204−206	385.9574/385.9572[c]
18a	Cl			1	68	108−109	589.9888/589.9881[b]
18b	Br			1	61	124−125	677.8878/677.8871[c]

[a] Yields referred to isolated and purified material. [b] ^{35}Cl isotope. [c] ^{79}Br isotope.

ones (8a,b−10a,b and 13a,b−14a,b). The alkyl-iodide or bromide (0.85 mmol) was added slowly to a solution of **7a** or **7b** (0.77 mmol). The reaction has been carried out at room temperature, in the dark and under magnetic stirring until disappearance of the starting **7a** or **7b**. The silver iodide or bromide were filtered off, and the solution evaporated under reduced pressure. The crude material was purified by flash chromatography (SiO_2, ethyl acetate:petroleum ether = 1:4 v/v as eluant). In every case, an analytical sample of crystalline compounds (yellow crystals) was obtained by crystallization from EtOH/H_2O.

3-(4-Halogenobenzoyl)-4-[(*Z*)-1-methyl-2-nonylvinyl]-1,2,4-oxadiazol-5(4*H*)-ones (11a,b). A suspension of **7a** or **7b** (0.77 mmol) in 1-iodononane (25.4 mmol) has been kept at room temperature, in the dark and under magnetic stirring until disappearance of starting **7a** or **7b**. The silver iodide was filtered off, and the solution was evaporated under reduced pressure. The crude material was purified by flash chromatography (SiO_2, ethyl acetate:petroleum ether = 1:8 v/v as eluant). In both case, an analytical sample of crystalline compounds (yellow crystals) was obtained by crystallization from EtOH/H_2O.

3-(4-Halogenobenzoyl)-4-[(*Z*)-2-(isobutylthio)-1-methylvinyl]-1,2,4-oxadiazol-5(4*H*)-ones (12a,b). A suspension of **7a** or **7b** (0.77 mmol) in 1-iodo-2-methylpropane (25.4 mmol) has been kept at room temperature, in the dark and under magnetic stirring until disappearance of the starting **7a** or **7b**. The silver iodide was filtered off, and the solution was evaporated under reduced pressure. The crude material was purified by chromatography (SiO_2, ethyl acetate:petroleum ether gradient from 1:8 v/v to 2:1 as eluant) to obtain three compounds. The first running band was identified as *E*-isomer (5%, yellow oil), the second one as the desired product **12a** or **12b** (yellow oil), the third one as the dithio derivative **18a** or **18b** (traces, < 2%).

3-(4-Chlorobenzoyl)-4-{(*Z*)-2-[(3,5-dinitro-2-thienyl)thio]-1-methylvinyl}-1,2,4-oxadiazol-5(4*H*)-one (15a). A solution of 2-bromo-2,5-dinitrothiophene (0.62 mmol) in DMF (2 mL) was added to a solution of **7a** (0.62 mmol) in DMF (8 mL) and left at room temperature in the dark for 6 days. The desired product **15a** was obtained by crystallization (yellow crystals from toluene) of the precipitated solid.

3-(4-Bromobenzoyl)-4-{(*Z*)-2-[(3,5-dinitro-2-thienyl)thio]-1-methylvinyl}-1,2,4-oxadiazol-5(4*H*)-one (15b). A solution of 2-bromo-2,5-dinitrothiophene (0.62 mmol) in DMF (2 mL) was added to a solution of **7b** (0.62 mmol) in DMF (8 mL) and left at room temperature in the dark for 6 days. The inorganic salt was filtered off, and the solution was poured into H_2O (20 mL) and extracted with ethyl ether (5 × 20 mL). The extracts were dried over Na_2SO_4 and the solvent removed. The crude material was purified by flash chromatography (SiO_2, ethyl acetate:petroleum ether = 1:3 v/v as eluant). Compound **15b** was obtained as a yellow solid. An analytical sample was obtained by crystallization from toluene (yellow crystals).

3-(4-Halogenobenzoyl)-4-[(*Z*)-1-methyl-2-(methylsulfinyl)vinyl]-1,2,4-oxadiazol-5(4*H*)-one (16a,b). 3-Chloroperbenzoic acid (0.4 mmol) was added to a solution of **8a** or **8b** (0.4 mmol) in CH_2Cl_2 (6 mL), keeping the temperature under control (25−30 °C). The solution was stirred until disappearance of **8a**,**b**. Further CH_2Cl_2 (10 mL) was added, and the whole was extracted with a solution 5% of Na_2SO_3 (2 × 5 mL) and then with a solution 5% of $NaHCO_3$ (2 × 5 mL). The organic layer was then dried over Na_2SO_4 and the solvent removed. The crude material was purified by flash chromatography (SiO_2, ethyl acetate:petroleum ether = 1:1 v/v as eluant). Compounds **16a**,**b** have been obtained as a white solid. An analytical sample of crystalline compound was obtained by crystallization from EtOH/H_2O.

3-(4-Halogenobenzoyl)-4-[(*Z*)-1-methyl-2-(methylsulfonyl)vinyl]-1,2,4-oxadiazol-5(4*H*)-ones (17a,b). 3-Chloroperbenzoic acid (0.8 mmol) was added to a solution of **8a** or **8b** (0.4 mmol) in CH_2Cl_2 (6 mL). Operating as above **17a**,**b** have been obtained as white solid together with a small amount of **16a**,**b** (yield 8%). An analytical sample of crystalline compound was obtained by crystallization from EtOH/H_2O.

4,4′-[Dithiodi(1*Z*)prop-1-ene-1,2-diyl]bis[3-(4-alogenobenzoyl)-1,2,4-oxadiazol-5(4*H*)-one] (18a,b). Iodine (0.40 mmol) was added, at room temperature in the dark, to a solution of **7a**,**b** (0.67 mmol) in $CHCl_3$ (16 mL). Immediately the solution turned violet and AgI precipitated. After an hour, the silver iodide was filtered off and the solution evaporated under reduced pressure. The crude material was purified by flash chromatography (SiO_2, ethyl acetate:petroleum ether = 1:4 v/v as eluant).

B. Functional Studies. For details, please see Supporting Information, Section S8.

C. Binding Experiments. For details, please see Supporting Information, Section S11.

D. Electrophysiological Experiments. For details, please see Supporting Information, Section S13.

E. Computational Methods: In Silico 3D Superimpositions.

FLAP is a recently developed algorithm suitable for describing proteins and ligands based on a common reference framework. Given the 3D structure of a molecule, with the GRID force-field,[6] the interaction energy between the molecule and a probe are calculated at different points in space. As a result, one has the so-called molecular interaction fields (MIF): the hydrophobic and hydrogen bonding interactions of the molecule with a virtual receptor are schematized by the probes and encoded into energy values assigned to the nodes of a grid built around each molecule. MIF are of central importance in the execution of the FLAP algorithm because, given two molecules, their MIF are used by FLAP to align one over the other. The first step of the FLAP procedure is the creation of a database: all the molecules imported will be referred to as ligand molecules. The ligand molecules are subjected to a fast conformational analysis, a reasonable number of conformations are generated, and each conformer is individually treated (in this application, up to 100 conformations were generated by FLAP). Some representative fields are extracted from the MIFs of the individual elements entered and stored in the database. Then, a molecular template is imported, the corresponding MIF are calculated with the program GRID, and again some representative fields are selected from the MIFs. All the heavy atoms of the molecule are classified as hydrophobic or hydrogen bonding hotspots and combined in quadruplets. A mathematical model is then created, containing all the distances between all the possible combinations of four hotspots of the template molecule. This information is stored in a "virtual" bit-string, making future computations much easier and quicker to complete and compare. The next step in the FLAP process would be finding the matches of the four hotspots of the individual ligands to those of the template. When four hotspots of the ligand molecule are found to fit over four hotspots of the template framework, a potentially favorable superposition has been detected. Of course, the process is iterative, and it will continue until all the template quadruplets are combined in all possible ways with all ligand quadruplets. Each time, a score associated to the two molecules and their common quadruplet of hotspots quantifies the overlap of the two MIFs. At the end of the process, only the best superposition of each ligand to each template is memorized. A conformational sampling guaranteed an adequate treatment of molecular flexibility. For **1**, the conformational analysis was carried out using 10 different conformations and repeating for each conformation the entire procedure described. For details, see also the Supporting Information.

Acknowledgment. Supported by grants from MUR: PRIN-2005, (2005034305_1) "Chemistry, reactivity and biological activity of nitrogen- and/or oxygen- and/or sulphur-containing heterocycles" and from the University of Bologna. The technical support of Dr. Gaetano Corda for binding experiments is gratefully acknowledged.

Supporting Information Available: Physical properties and spectroscopic data for the compounds **7a**,**b**−**18a**,**b**, functional assays, receptor binding studies, electrophysiological experiments, and computational methods. This material is available free of charge via the Internet at http://pubs.acs.org.

References

(1) Triggle, D. J. Calcium Channel Antagonists: Clinical Uses-Past, Present, and Future. *Biochem. Pharmacol.* **2007**, *74*, 1–9.

(2) Striessnig, J. Pharmacology, Structure and Function of Cardiac L-type Ca(2+) Channels. *Cell. Physiol. Biochem.* **1999**, *9*, 242–269.

(3) Budriesi, R.; Cosimelli, B.; Ioan, P.; Lanza, C. Z.; Spinelli, D.; Chiarini, A. Cardiovascular Characterization of [1,4]Thiazino[3,4-*c*][1,2,4]oxadiazol-1-one-derivatives: Selective Myocardial Calcium Channel Modulators. *J. Med. Chem.* **2002**, *45*, 3475–3481.

(4) Budriesi, R.; Carosati, E.; Chiarini, A; Cosimelli, B.; Cruciani, G.; Ioan, P.; Spinelli, D.; Spisani, R. A New Class of Selective Myocardial Calcium Channel Modulators. 2. The Role of the Acetal Chain in Oxadiazol-3-one Derivatives. *J. Med. Chem.* **2005**, *48*, 2445–2456.

(5) Campiani, G.; Garofalo, A.; Fiorini, I.; Botta, M.; Nacci, V.; Tafi, A.; Chiarini, A.; Budriesi, R.; Bruni, G.; Romeo, M. R. Pyrrolo[2,1-*c*][1,4]benzothiazines: Synthesis, Structure−Activity Relationships, Molecular Modeling Studies and Cardiovascular Activity. *J. Med. Chem.* **1995**, *38*, 4393–4410.

(6) (a) Goodford, P. J. A Computational Procedure for Determining Energetically Favorable Binding Sites on Biologically Important Macromolecules. *J. Med. Chem.* **1985**, *28*, 849–857. (b) Carosati, E.; Sciabola, S.; Cruciani, G. Hydrogen Bonding Interactions of Covalently Bonded Fluorine Atoms: From Crystallographic Data to a New Angular Function in the GRID Force Field. *J. Med. Chem.* **2004**, *47*, 5114–5125. (c) *GRID, v. 22 for Linux*; Molecular Discovery Ltd.: 215 Marsh Road, HA5 5NE Pinner, Middlesex, UK; http://www.moldis-covery.com.

(7) Hu, H.; Marban, E. Isoform-Specific Inhibition of L-Type Calcium Channel by Dihydropyridines is Independent of Isoform-Specific Gating Properties. *Mol. Pharmacol.* **1998**, *53*, 902–907.

(8) Marionneau, C.; Couette, B.; Liu, J.; Li, H.; Mangoni, M. E.; Nargeot, J.; Lei, M.; Escande, D.; Demolombe, S. Specific Pattern of Ionic Channel Gene Expression Associated with Pacemaker Activity in the Mouse Heart. *J. Physiol.* **2005**, *562*, 223–234.

(9) Carosati, E.; Cruciani, G.; Chiarini, A.; Budriesi, R.; Ioan, P.; Spisani, R.; Spinelli, D.; Cosimelli, B.; Fusi, F.; Frosini, M.; Matucci, R.; Gasparrini, F.; Ciogli, A.; Stephens, P. J.; Devlin, F. J. New Calcium Channel Antagonists Discovered by a Multidisciplinary Approach. *J. Med. Chem.* **2006**, *49*, 5206–5216.

(10) Carosati, E.; Budriesi, R.; Ioan, P.; Ugenti, M. P.; Frosini, M.; Fusi, F.; Corda, G.; Cosimelli, B.; Spinelli, D.; Chiarini, A.; Cruciani, G. Discovery of Novel and Cardioselective Diltiazem-like Calcium Channel Blockers via Virtual Screening. *J. Med. Chem.* **2008**, *51*, 5552–5565.

(11) Budriesi, R.; Cosimelli, B.; Ioan, P.; Carosati, E.; Ugenti, M. P.; Spisani, R. Diltiazem Analogues: the Last Ten Years on Structure−Activity Relationships. *Curr. Med. Chem.* **2007**, *14*, 279–287.

(12) Tallarida, R. J.; Murray, R. B. *Manual of Pharmacologic Calculations with Computer Programs*, 2nd ed.; Springer-Verlag: New York, 1987.

(13) Motulsky, H., Christopoulos, A. *Fitting Models to Biological Data Using Linear and Nonlinear Regression*, 2003; www.graphpad.com.

(14) Motulsky H., *Statistic Guide: Statistical Analysis for Laboratory and Clinical Research. A Practical Guide to Curve Fitting*, 2003; www.graphpad.com.

(15) (a) Anslyn, E. V.; Dougherty, D. A. *Modern Physical Organic Chemistry*; University Science Books: Sausalito, CA, 2004; p 72. (b) Isaacs, N. S. *Physical Organic Chemistry*; Longman Scientific and Technical: Harlow, Essex, UK 1987; p 37.

(16) Solomons, T. W. G.; Fryhle, C. B. *Organic Chemistry*; J. Wiley & Sons: New York, 2007; Chapter 22.

(17) Anslyn, E. V.; Dougherty, D. A. *Modern Physical Organic Chemistry*; University Science Books: Sausalito, CA, 2004; p 545.

(18) Crampton, M. R. Acidity and hydrogen bonding. In *The Chemistry of the Thiol Group*; Patai, S., Ed.; J. Wiley & Sons: New York, 1974; part 1, Chapter 8.

(19) Anslyn, E. V.; Dougherty, D. A. *Modern Physical Organic Chemistry*; University Science Books: Sausalito, CA, 2004; pp 637−638.

(20) Terrier, F. *Nucleophilic Aromatic Displacement: The Influence of the Nitro Group*; Feuer H., Ed.; VCH:: New York, 1991; pp 29−36.

(21) Peach, M. E. Thiols as nucleophiles. In *The Chemistry of the Thiol Group*; Patai, S., Ed.; J. Wiley & Sons: New York, 1974; part 2, Chapter 16.

(22) (a) Cornils, B.; Herrmann, W. A.; Schlögl, R.; Wong, C.-H.; *Catalysis from A to Z—A Concise Encyclopedia*; Wiley VCH: Weinheim, 2003; p 824; (b) *March's Advanced Organic Chemistry: Reactions, Mechanisms and Structure*; Smith, M. B., March, J., Eds.; Wiley VCH: Weinheim, 2007; Chapter 10.

(23) Oba, T.; Aoki, T.; Koshita, M.; Nihonyanagi, K.; Yamaguchi, M. Muscle Contraction and Inward Current Induced by Silver and Effect of Ca^{2+} Channel Blockers. *Am. J. Physiol.* **1993**, C852–C856.

(24) Tupling, R.; Green, H. Silver Ions Induce Ca^{2+} Release from the SR In Vitro by Acting on the Ca^{2+} Release Channel and the Ca^{2+} Pump. *J. Appl. Physiol.* **2002**, *4*, 1603–1610.

(25) Gubin, J.; Lucchetti, J.; Mahaux, J.; Nisato, D.; Rosseels, G.; Clinet, M.; Polster, P.; Chatelain, P. A Novel Class of Calcium-Entry Blockers: the 1[[4-(Aminoalkoxy)phenyl]sulfonyl]indolizines. *J. Med. Chem.* **1992**, *35*, 981–988.

(26) Gubin, J.; de Vogelaer, H.; Inion, H.; Houben, C.; Lucchetti, J.; Mahaux, J.; Rosseels, G.; Peiren, M.; Clinet, M.; Polster, P.; Chatelain, P. Novel Heterocyclic Analogues of the New Potent Class of Calcium Entry Blockers: 1-[[4-(Aminoalkoxy)phenyl]sulfonyl]indolizines. *J. Med. Chem.* **1993**, *36*, 1425–1433.

(27) Spinelli, D.; Mugnoli, A.; Andreani, A.; Rambaldi, M.; Frascari, S. New Ring Transformation: Conversion of 6-*p*-Chlorophenyl-3-methyl-5-nitrosoimidazo[2,1-*b*]thiazole into 8-*p*-Chlorophenyl-8-hydroxy-5-methyl-3-oxo-1,2,4-oxadiazolo[3,4-*c*][1,4]thiazine by the

Action of Mineral Acids. *J. Chem. Soc., Chem. Commun.* **1992**, 1394–1395.
(28) Andreani, A.; Billi, R.; Cosimelli, B.; Mugnoli, A.; Rambaldi, M.; Spinelli, D. Ring-Ring Interconversion: the Rearrangement of 6-(4-Chlorophenyl)-3-methyl-5-nitrosoimidazo[2,1-*b*][1,3]thiazole into 8-(4-Chlorophenyl)-8-hydroxy-5-methyl-8*H*-[1,4]thiazino[3,4-*c*][1,2,4]oxadiazol-3-one. Elucidation of the Reaction Product through Spectroscopic and X-Ray Crystal Structure Analysis. *J. Chem. Soc., Perkin Trans.* **1997**, *2*, 2407–2410.
(29) Exner, O. *Correlation Analysis of Chemical Data*; Plenum Press: New York and London, 1988.
(30) Tikhonov, D. B.; Zhorov, B. S. Benzothiazepines in L-type Calcium Channel: Insights from Molecular Modelling. *J. Biol. Chem.* **2008**, *283*, 17594–17604.
(31) Baroni, M.; Cruciani, G.; Sciabola, S.; Perruccio, F.; Mason, J. S. A Common Reference Framework for Analyzing/Comparing Proteins and Ligands. Fingerprints for Ligands And Proteins (FLAP): Theory and Application. *J. Chem. Inf. Model.* **2007**, *47*, 279–294.
(32) DeLano, W. L. *The PyMOL Molecular Graphics System*; DeLano Scientific LLC: Palo Alto, CA, 2008; http://www.pymol.org.
(33) Richardson, P.; McKenna, W.; Bristow, M.; Maisch, B.; Mautner, B.; O'Connell, J.; Olsen, E.; Thiene, G.; Goodwin, J.; Gyarfas, I.; Martin, I.; Nordet, P. Report of the 1995 World Health Organization/International Society and Federation of Cardiology Task Force on the Definition and Classification of Cardiomyopathies. *Circulation* **1996**, *93*, 841–842.
(34) Maron, B. Hypertrophic cardiomyopathy: a systematic review. *JAMA, J. Am. Med. Assoc.* **2002**, *287*, 1308–1320.
(35) Smith, S. C., Jr.; Spector, S. L. Cardioselective beta-adrenergic therapy in a patient with asthma and hypertrophic obstructive cardiomyopathy. *Chest* **1981**, *80*, 103–105.
(36) Billi, R.; Cosimelli, B.; Spinelli, D.; Rambaldi, M. Ring-Ring Interconversions. Part 2. Effect of Substituents on the Rearrangement of 6-Aryl-3-methyl-5-nitrosoimidazo[2,1-*b*][1,3]thiazoles to 8-Aryl-8-hydroxy-5-methyl-8*H*-[1,4]thiazino[3,4-*c*][1,2,4]oxadiazol-3-ones. A Novel Class of Potential Antitumor Agents. *Tetrahedron* **1999**, *55*, 5433–5440.

JM801351U